

# Manuscript Title: Measurement of the continuous Lehmann rotation of cholesteric droplets subjected to a temperature gradient

Patrick Oswald\* and Alain Dequidt  
*Université de Lyon, Laboratoire de Physique,  
 École Normale Supérieure de Lyon, CNRS,  
 46 Allée d'Italie, 69364 Lyon, France.*

(Dated: January 9, 2009)

In 1900, Otto Lehmann observed the continuous rotation of cholesteric drops when subjected to a temperature gradient. This thermomechanical phenomenon was predicted 68 years later by Leslie from symmetry arguments but was never reobserved to our knowledge. In this letter, we present an experiment allowing quantitative analysis of the Lehmann effect at the cholesteric-isotropic transition temperature. More precisely, we measure the angular velocity of cholesteric drops as a function of their size and the temperature gradient and we show that applying an electric field can stop the drop rotation. From these observations and a theoretical model we estimate the Lehmann coefficient  $\nu$ .

PACS numbers: 61.30.-v, 05.70.Ln, 65.40.De

In a nematic liquid crystal, the rod-like molecules tend to align along a single direction  $\vec{n}$  called director. If one adds chiral molecules to a nematic phase, one obtains a cholesteric phase in which  $\vec{n}$  rotates around a space direction called the helical axis. In 1900, Otto Lehmann observed that the internal texture of drops of a cholesteric liquid crystal spread out between two glass plates could be put into motion when heated from below [1]. This work was completed in a book published in 1921 [2]. Although this phenomenon was predicted 68 years later by Leslie [3] from symmetry arguments, the Lehmann experiment was never reproduced to our knowledge. This is frustrating as this observation is certainly one of the most spectacular effects of chirality in hydrodynamics. As proof the number of purely theoretical articles dealing with this effect [4–8], including recent molecular dynamics simulations [9]. In this article, we fill this experimental gap by presenting a new experiment allowing us to quantitatively analyze the original Lehmann effect in the framework of the Leslie theory.

In order to succeed in this delicate experiment, the director must be free to rotate at the boundaries of the drops. For this purpose, we realized a  $25\ \mu\text{m}$ -thick cell made of two parallel glass plates treated for planar sliding anchoring. The latter was obtained by spin coating a thin layer of the polymercaptan hardener of an epoxy resin (Structuralit 7) (for more details, see Ref. [10]). Note that we did not observe the Lehmann rotation on bare glass nor when it was treated for planar anchoring with a polyimide or for homeotropic anchoring. The cholesteric liquid crystal chosen is a mixture of 4-n-octyloxy-4'-cyanobiphenyl (8OCB from Synthron Chemicals GmbH & Co) and of cholesteryl chloride (CC

from Aldrich) in proportion 1:1 in weight. It starts to melt at  $66^\circ\text{C}$  with a freezing range of about  $0.6^\circ\text{C}$ . In order to impose a vertical temperature gradient to the sample, the cell is sandwiched between two transparent ovens regulated in temperature within  $\pm 0.01^\circ\text{C}$  owing to two separated recirculating water baths. Two thin layers of glycerol are introduced between the cell and the ovens in order to improve thermal contacts. We checked that the sample temperature was given by  $(T_b + T_t)/2$  within  $\pm 0.1^\circ\text{C}$  whatever the temperatures chosen for the bottom and top ovens ( $T_b$  and  $T_t$ , respectively). A polarizing Leica microscope and a video camera (Pike F 145B) allow us to observe the sample and to capture up to 30 images/s with a resolution of  $1380 \times 1024$  pixels. Our setup is represented in Fig. 1. In the following, we shall denote by  $\Delta T$  the difference  $T_b - T_t$ . This quantity is directly proportional to the imposed temperature gradient  $G$  which will be evaluated later.

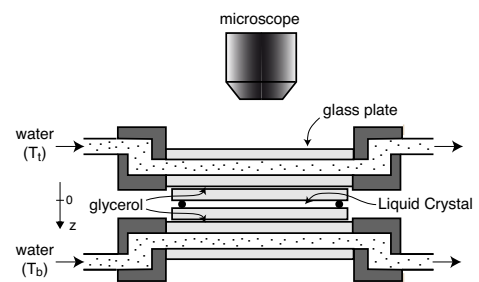


FIG. 1: Experimental setup. The  $z$  axis is vertically oriented towards the bottom so that  $G > 0$  when  $T_b > T_t$ .

Our experiment consisted of imposing a  $\Delta T$  in order that the sample temperature remained always very close to its solidus temperature. Under these conditions, small drops of cholesteric phase form and coexist with the isotropic liquid. These drops partially wet the colder glass plate. They are circular with a banded texture in-

\*Electronic address: [patrick.oswald@ens-lyon.fr](mailto:patrick.oswald@ens-lyon.fr)

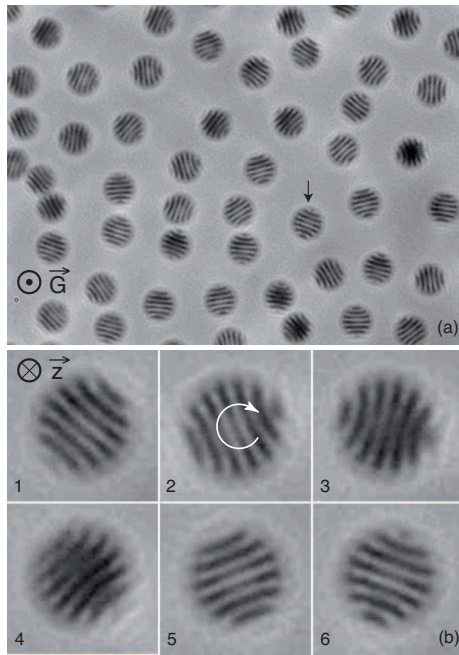


FIG. 2: a) Germs observed in natural light; b) Sequence of pictures showing the rotation of the drop marked by an arrow in (a). For this temperature gradient all the drops rotate clockwise:  $\Delta T = -6.3^\circ\text{C}$ ,  $D \approx 12.5 \mu\text{m}$  and  $\omega = 0.042\text{rd/s}$ .

side which rotates at constant angular velocity as can be seen in Fig. 2. In this sequence, all pictures were taken in natural light so that the drop contrast (largely enhanced in this figure) did not change in time. We checked experimentally that the drops rotate in the opposite direction when the sign of the temperature gradient is reversed.

To measure precisely the rotation period of the drops  $\Theta$ , we defocussed them under the microscope in order that their striations be no longer visible and we added a polarizer. In this way, each drop forms a spot the intensity of which depends on the bands orientation with respect to the light polarization. More precisely, the drops appears white when the bands are parallel to the polarization and black when they are perpendicular. The next step was to record a sequence of images of several drops over several periods. From this sequence, we calculated the autocorrelation function  $C(t)$  of the image taken at time  $t$  with that taken at time  $t = 0$ :  $C(t) = \sum_{i=1}^n [I_i(t)I_i(0)]/n$  where  $I_i(t)$  is the intensity of the  $i$ -th pixel (each image was normalized in order that  $\sum_{i=1}^n I_i(t) = 0$ ). This function is plotted as a function of time in Fig. 3. It oscillates with a period equal to the half period of rotation of the drops.

In order to test the influence of the drop size on the rotation velocity, we increased by a few hundredths of a degree the sample temperature while maintaining a constant temperature gradient. In this way, we were able to change the drop diameter between typically 3 and  $10 \mu\text{m}$ . In this diameter range, the drops were separated and well visible under the microscope. On the other hand, we did not succeed in obtaining bigger drops because of their

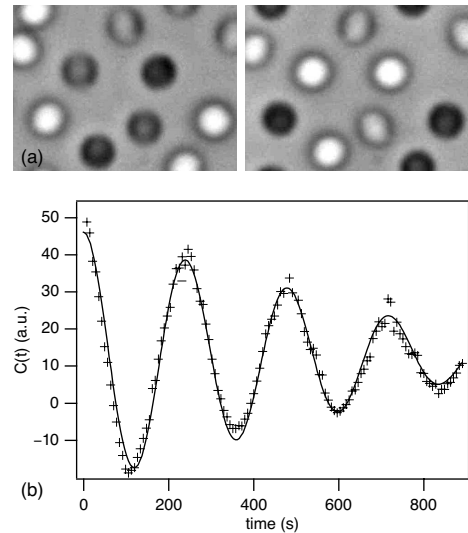


FIG. 3: a) Germs observed in polarized light after defocussing. They appear as black or white spots depending on whether their internal bands are parallel or perpendicular to the light polarization; b) Autocorrelation function  $C(t)$ . Its period gives the half-period of rotation of the drops. The solid line is a fit to a cosine function, the amplitude of which decreases linearly with time.  $\Delta T = 2.7^\circ\text{C}$ .

tendency to continuously merge which makes impossible any quantitative measurement. In Fig. 4, the rotation period  $\Theta$  is plotted as a function of the drop diameter  $D$  for an intermediate gradient ( $\Delta T_i = 14.65^\circ\text{C}$ ). This curve shows that the period systematically increases when the diameter increases. In addition, it is well fitted with a law of type  $a + bD^2$ . This dependence will be justified later.

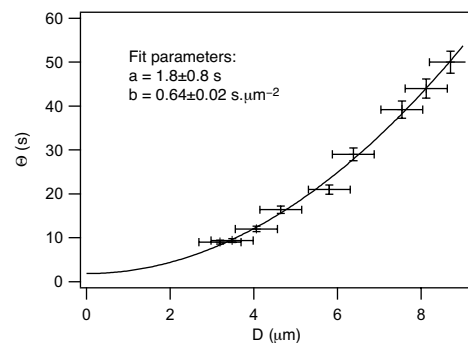


FIG. 4: Period of rotation of the drops (in absolute value) as a function of their diameter ( $\Delta T = 14.65^\circ\text{C}$ ). Note that for this temperature gradient, the drops rotate anticlockwise which means that their angular velocity is negative with our conventions.

We then analyzed the temperature gradient dependence of the rotation frequency  $f = 1/\Theta$ . This study was performed by varying  $\Delta T$ . In these experiments, it was difficult to keep the drop size constant (the larger  $\Delta T$ , the smaller the drops in general). For this reason, we measured frequency  $f$  for each  $\Delta T$  once the drops

were well separated and all of the same size, without worrying about their diameter. We then renormalized the measured frequency by the frequency found at  $\Delta T_i$  for drops of similar diameter. The dimensionless frequency  $f_{norm} = f \times (a + bD^2)$  is plotted in Fig. 5 as a function of  $\Delta T$ . It is well fitted with a linear law. This dependence shows that the drops rotate with an angular velocity  $|\omega| = 2\pi f$  proportional to the temperature gradient (with  $\omega$  and  $G$  of opposite signs in our experiments).

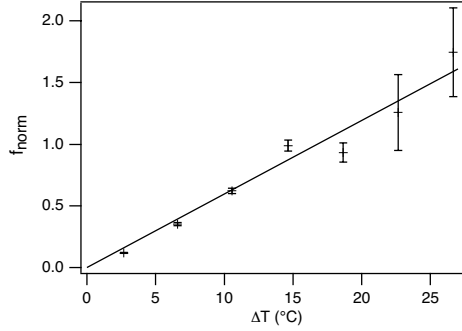


FIG. 5: Normalized rotation frequency as a function of the temperature difference.

In order to explain these observations, we must solve the torque equation. Neglecting backflow effects ( $\vec{v} = 0$ ), a point we shall return to later, this equation reads [11, 12]

$$\gamma_1 \frac{\partial \vec{n}}{\partial t} = \vec{h} + \nu \vec{n} \times \vec{G} \quad (1)$$

where  $\vec{G} = \vec{\nabla}T$  is the temperature gradient,  $\vec{h} = -\frac{\delta f_e}{\delta \vec{n}}$  the molecular field (with  $f_e$  the usual Frank elastic energy),  $\gamma_1$  the rotational viscosity and  $\nu$  the Lehmann coefficient introduced for the first time by Leslie in 1968 [3]. Because the texture does not change in time, the total elastic energy of the drop  $F = \iiint_{\text{drop}} f_e dV$  is constant. As a consequence, we can write:

$$\frac{dF}{dt} = \iiint_{\text{drop}} \frac{\delta f_e}{\delta \vec{n}} \cdot \frac{\partial \vec{n}}{\partial t} dV = - \iiint_{\text{drop}} \vec{h} \cdot \frac{\partial \vec{n}}{\partial t} dV = 0 \quad (2)$$

Taking the scalar product of Eq. 1 with  $\frac{\partial \vec{n}}{\partial t}$  and integrating over the drop, we obtain by using Eq. 2:

$$\gamma_1 \iiint_{\text{drop}} \left( \frac{\partial \vec{n}}{\partial t} \right)^2 dV = \nu \vec{G} \cdot \iiint_{\text{drop}} \frac{\partial \vec{n}}{\partial t} \times \vec{n} dV \quad (3)$$

If the texture rotates at a constant angular velocity  $\vec{\omega} = \omega \vec{e}_z$ , it can be shown that the director rotates in place in such a way that

$$\frac{\partial \vec{n}}{\partial t} = \omega \vec{e}_z \times \vec{n} - \omega \frac{\partial \vec{n}}{\partial \theta} \quad (4)$$

where  $\theta$  is the polar angle. Finally, one obtains from the

two previous equations

$$-\frac{\nu G}{\gamma_1 \omega} = 1 + \frac{\iiint_{\text{drop}} \left[ \vec{e}_z \cdot \frac{\partial \vec{n}}{\partial \theta} \times \vec{n} + \left( \frac{\partial \vec{n}}{\partial \theta} \right)^2 \right] dV}{\iiint_{\text{drop}} \left[ \vec{e}_z \cdot \frac{\partial \vec{n}}{\partial \theta} \times \vec{n} + 1 - (\vec{e}_z \cdot \vec{n})^2 \right] dV} \quad (5)$$

This equation shows that the texture angular velocity is proportional to  $G$ , in agreement with experiments, and has the form  $\omega = -A\nu G/\gamma_1$  where  $A$  is a dimensionless coefficient which depends on the director field and on the drop geometry.

In order to estimate this coefficient, we assume that the director field remains topologically unchanged whatever the velocity  $\omega$ . In our experiments, due to the temperature gradient, the drops wet the coldest glass plate. They are also flattened by the thermal gradient in the same way as a macroscopic drop subjected to the action of gravity. For this reason, we will model the drop as a flat cylindrical box of height  $h$  and diameter  $D$ . We now need to specify the director field. On the glass (situated at  $z = 0$  when  $G > 0$ , see Fig. 1), the anchoring is planar and gliding. In contact with the isotropic liquid (at  $z = h$ ), the banded texture indicates that the anchoring is rather homeotropic, which we shall assume in the following. Under these conditions, we know from previous work [13] that the director field has the form

$$\begin{aligned} n_x &= \cos \beta \sin \gamma \sin ky - \cos \alpha \sin \beta \sin \gamma \cos ky \\ &\quad + \sin \alpha \sin \beta \cos \gamma \\ n_y &= -\sin \beta \sin \gamma \sin ky - \cos \alpha \cos \beta \sin \gamma \cos ky \\ &\quad + \sin \alpha \cos \beta \cos \gamma \\ n_z &= \sin \alpha \sin \gamma \cos ky + \cos \alpha \cos \gamma \end{aligned} \quad (6)$$

where  $\beta = -\frac{qh}{K_{32}} \left( \frac{z}{h} - \frac{1}{2} \right)$  (with  $K_{32}$  the ratio of the bend over the twist elastic constants and  $q = 2\pi/P$  the equilibrium twist),  $\alpha = \frac{\pi}{2} \left( 1 - \frac{z}{h} \right)$  and  $\gamma = \varepsilon \sin \left( \pi \frac{z}{h} \right)$  with  $\varepsilon \ll 1$ . We recall that this solution corresponds to a modulation of amplitude  $\varepsilon$  and of wave vector  $k$  along the  $y$  axis of the well-known TIC (for Translationally Invariant Configuration) [14]. Calculation at second order in  $\varepsilon$  of the integrals in Eq. 5 yields

$$-\frac{\nu G}{\gamma_1 \omega} = 1 + \frac{1}{16} k^2 \varepsilon^2 D^2 \quad (7)$$

We note that at this order, the result does not explicitly depend on  $K_{32}$  nor on the drop height  $h$ . More important is that  $\omega$  is independent of  $D$  when  $k = 0$  which is normal as the director field corresponds to the TIC in this limit. This shows that the band texture is responsible for the decrease of  $\omega$  when  $D$  increases. Another crucial point is that backflow disappears when  $k \rightarrow 0$  (TIC limit) or when  $D \rightarrow 0$  (i.e. when the drop diameter is much smaller than the pitch). This indicates that backflow effects must only enter into the prefactor of  $k^2 \varepsilon^2 D^2$  in Eq. 7. For this reason, the extrapolation to  $D = 0$  of the curve  $\Theta(D)$  shown in Fig. 4 must directly

give the ratio  $\nu/\gamma_1$  in spite of the fact we have neglected backflow. In experiments, the periodicity and the optical contrast of the bands do not change in a noticeable way as a function of the drop diameter, suggesting that both  $k$  and  $\varepsilon$  are constant. In this case, Eq. 7 is compatible with experiments as it predicts not only that the angular velocity  $\omega$  is proportional to the temperature gradient  $G$ , but also that the rotation period  $\Theta$  is quadratic in the drop diameter  $D$ . Note, in addition, that the Lehmann coefficient  $\nu$  is positive in our liquid crystal as  $\omega$  and  $G$  are of opposite sign. In order to estimate the value of the ratio  $\nu/\gamma_1$ , we extrapolate to  $D = 0$  the rotation period measured as a function of  $D$  at the intermediate temperature gradient  $G_i \propto \Delta T_i$  (Fig. 4). Doing this, we obtain  $\frac{\nu}{\gamma_1} = \frac{2\pi}{aG_i}$  where  $a$  is the fit parameter. As for  $G_i$ , it is given by  $\frac{\Delta T_i}{4e} \frac{\kappa_g}{\kappa_{LC}}$ , where  $e$  is the thickness of each glass plate (1mm, see Fig. 1) and  $\kappa_g$  (resp.  $\kappa_{LC}$ ) the thermal conductivity of the glass (resp. of the liquid crystal). Note that we neglect here the influence of the glycerol and liquid crystal layers as they are much thinner than the glass plates (about  $25\mu\text{m}$  each to be compared to 1mm). In practice, we measured the ratio  $\kappa_g/\kappa_{LC}$  by replacing the upper glycerol layer by a layer of pure 8OCB. The latter has a nematic-to-smectic A phase transition at temperature  $T_{NA} = 67^\circ\text{C}$ . This transition is easy to detect under the microscope. It can therefore be used as a reference temperature. The method to measure the conductivity ratio was thus to impose different temperatures  $T_b$  and  $T_t$  while maintaining the temperature of the 8OCB layer exactly at  $T_{NA}$ . To increase the sensibility of the measurement, we also used a  $500\mu\text{m}$ -thick sample of the 8OCB-CC mixture. In this way, we obtained  $\kappa_g/\kappa_{LC} \approx 7$  which gives  $G_i \approx 26^\circ\text{C}/\text{mm}$ . As  $a \sim 2\text{s}$ , we finally calculate  $\frac{\nu}{\gamma_1} \sim 1 \times 10^{-4}\text{s}^{-1}\text{K}^{-1}\text{m}$ .

In order to directly estimate the value of  $\nu$ , we performed another experiment consisting of submitting the cholesteric drops to an electric field parallel to the glass plates. Doing this we observed that the drops stop rotating above a critical electric field  $E_c$  which is independent of their size. In this case, the Lehmann torque is equilibrated by the dielectric torque. A straightforward calculation yields:

$$\nu = f \frac{\varepsilon_0 \varepsilon_a E_c^2}{2G} \quad (8)$$

where  $\varepsilon_a$  is the dielectric anisotropy and  $f$  a dimensionless factor of order unity which depends on the structure of the director field inside the droplet ( $f = 1$  to first order in  $\varepsilon$  by using the director field given in Eq. 6). Experimentally, we measured  $E_c \approx 7 \times 10^4 \text{V/m}$  (at frequency 10 kHz) for a temperature gradient  $G = 50^\circ\text{C}/\text{mm}$ . Taking  $\varepsilon_a \sim 3.5$  at the transition temperature, we calculate  $\nu \sim 1.5 \times 10^{-6} \text{kgK}^{-1}\text{s}^{-2}$  from Eq. 8. This allows us to estimate the rotational viscosity at the transition temperature:  $\gamma_1 \sim 0.015 \text{Pa.s}$ .

The value of  $\nu$  is typically 5 times larger than the value we measured by a static method in the same mixture about  $7.5^\circ\text{C}$  below the melting point, at the compensation temperature [15]:  $\nu \approx 2.8 \times 10^{-7} \text{kgK}^{-1}\text{s}^{-2}$  [16]. This shows that the Lehmann coefficient increases when the temperature increases. As for  $\gamma_1$ , it decreases (as expected from the comparison with other materials [17]) from  $0.075 \text{Pa.s}$  at the compensation temperature to about  $0.015 \text{Pa.s}$  at the melting point.

Experiments at other concentrations of CC and with other chiral dopants are now in progress to better understand the Lehmann effect.

- 
- [1] O. Lehmann, *Ann. Phys. Leipzig* **2**, 649 (1900).
  - [2] O. Lehmann, *Flüssige Kristalle und ihr Scheinbares Leben* (Verlag von Leopold Voss, Leipzig 1921).
  - [3] F. M. Leslie, *Proc. R. Soc. London Ser. A* **307**, 359 (1968).
  - [4] J. Prost, *Solid State Commun.* **11**, 183 (1972).
  - [5] H. K. Jayaram, U. D. Kini, G. S. Ranganath, and S. Chandrasekhar, *Mol. Cryst. Liq. Cryst.* **99**, 155 (1983).
  - [6] G. S. Ranganath, *Mol. Cryst. Liq. Cryst. Lett.* **92**, 105 (1983).
  - [7] F. M. Leslie, *J. Non-Equilib. Thermodyn.* **11**, 23 (1986).
  - [8] H. R. Brand and H. Pleiner, *Phys. Rev. A* **37**, 2736 (1988).
  - [9] S. Sarman, *Mol. Phys.* **99**, 1235 (2001).
  - [10] P. Oswald, A. Dequidt, and A. Żywociński, *Sliding planar anchoring and viscous surface torque in a cholesteric liquid crystal* (accepted to *Phys. Rev. E*).
  - [11] P. G. de Gennes, *The Physics of Liquid Crystals* (Clarendon Press, Oxford 1974), p. 97.
  - [12] P. Oswald and P. Pieranski, *Nematic and Cholesteric Liquid Crystals: Concepts and Physical Properties Illustrated by Experiments* (Taylor & Francis, CRC press, Boca Raton 2005), p. 486.
  - [13] J. Baudry, M. Brazovskaia, L. Lejcek, P. Oswald, and S. Pirkl, *Liq. Cryst.* **21**, 893 (1996).
  - [14] The meaning on the unit sphere  $S^2$  of angles  $\alpha$ ,  $\beta$ , and  $\gamma$  is given in Fig. BVII.44 of Ref. [12] p. 463.
  - [15] We recall that the equilibrium twist vanishes and changes sign at the compensation temperature.
  - [16] A. Dequidt, A. Żywociński, and P. Oswald, *Eur. Phys. J. E* **25**, 277 (2008).
  - [17] H. Kneppel, F. Schneider, and N. K. Sharma, *J. Chem. Phys.* **77**, 3203 (1982).